



**CHALMERS**

---

CPL

*Chalmers Publication Library*

Institutional Repository of  
Chalmers University of Technology  
<http://publications.lib.chalmers.se>

---

### **Copyright notice (preprint)**

This is a preprint of an article whose final and definitive form has been published in *Applied Catalysis B - Environmental*. Copyright© 2011 Elsevier. The published article is available online at: <http://dx.doi.org/10.1016/j.apcatb.2011.02.026>



1  
2  
3  
4  
5  
6  
7  
8  
9  
10  
11  
12  
13  
14  
15  
16  
17  
18  
19  
20  
21  
22

**Abstract**

This study focuses on lean NO<sub>x</sub> reduction (LNR) by *n*-octane using silver-alumina based catalysts, with the addition of hydrogen. The work takes a system approach, where parameters such as temperature, reformat gas composition, fuel penalty and realistic monolith samples are considered. The LNR catalyst samples were prepared by impregnation and sol-gel methods and the NO<sub>x</sub> reduction performance was characterized by flow-reactor experiments, where realistic engine-out gas compositions were used. The hydrogen feed over the LNR catalyst samples was determined via data achieved by autothermal reforming experiments over a rhodium based catalyst, using real diesel as feedstock. The LNR catalyst samples generally show an enhanced NO<sub>x</sub> reduction when hydrogen is added to the gas feed. In particular, a 2 wt% silver-alumina sample with the addition of minute amounts of platinum, shows a high increase in NO<sub>x</sub> reduction when hydrogen is added to the feed. The addition of CO, a potential poison in the reaction and a by-product from the reforming, did not show any significant effect on the LNR catalyst performance at the conditions used. This is beneficial, since it renders a CO clean-up step in the reformer system unneeded. Ammonia formation is discussed in terms of a possible dual-SCR system. Finally, the fuel penalty for hydrogen production and hydrocarbon addition is taken into consideration. It is found that an addition of 1000 ppm H<sub>2</sub> leads to unacceptable fuel penalties.

*Keywords:* Lean NO<sub>x</sub> reduction, Ag/Al<sub>2</sub>O<sub>3</sub>, Pt, fuel reforming, fuel economy.

1

## 2 **1. Introduction**

3 Combustion in excess oxygen, as in diesel- and lean-burn engines, can significantly improve the  
4 fuel economy for automotive engines, thus reducing the formation of CO<sub>2</sub>. However, the lean  
5 environment in the exhaust gas obstructs the ability of the conventional three-way catalyst to  
6 reduce NO<sub>x</sub>. New strategies for efficient lean NO<sub>x</sub> reduction must therefore be developed. In  
7 connection to this, fuel cell auxiliary power (FC-APU) and hydrocarbon selective catalytic  
8 reduction (HC-SCR or LNR) units are proposed as two major strategies as ground for introducing  
9 hydrogen in the transport sector to reduce emissions.

10

11 A promising catalyst for HC-SCR is silver-alumina [1-7], over which high conversion of NO<sub>x</sub> to  
12 N<sub>2</sub> with hydrocarbons as reductant has been demonstrated [2, 7-13]. However, poor performance  
13 at low temperatures, typically 150–300 °C, is a drawback since efficient NO<sub>x</sub> abatement at these  
14 temperatures is required for *e.g.* diesel engine exhausts. By using long-chained hydrocarbons the  
15 SCR reaction has previously been shown to proceed at lower temperatures and with wider  
16 activity window, compared to using shorter hydrocarbons [11, 14, 15]. The reason for this effect  
17 is suggested to be related to the lower activation (*i.e.* partial oxidation) temperature for longer  
18 hydrocarbons, compared to shorter ones [15, 16]. Furthermore, results show that the addition of  
19 small amounts of hydrogen drastically improves the low-temperature activity, first reported by  
20 Satokawa [17] in 2000.

21

22 On-board fuel processing of liquid hydrocarbon fuels is a way to supply hydrogen to a vehicle by  
23 using the existing fuel infra-structure. The hydrogen can be used either for avoiding operation of  
24 a truck engine at stand-still by using an APU system, or to increase the low-temperature activity

1 of silver-based NO<sub>x</sub> reduction catalysts. The latter option will be discussed in this paper. An FC-  
2 APU system could also be used in marine applications or as a range extender in a fuel cell  
3 vehicle. The critical step in the reforming process is the evaporation and catalytic conversion of  
4 the hydrocarbon fuel into a hydrogen-rich reformat. Rh-based monolithic catalysts have proven  
5 to be very active for autothermal reforming (ATR) of diesel [18]. Furthermore, these catalysts  
6 have showed a high selectivity and a good durability while using commercial diesel fuels.  
7  
8 Limited number of studies can be found in the open literature where the performance of a HC-  
9 SCR catalyst has been investigated using both diesel reformat and exhaust gas as feedstocks [19,  
10 20]. Along with hydrogen production also carbon monoxide is formed in the reformer system.  
11 For use in e.g. a polymer electrolyte fuel cell (PEFC) based APU system, high CO levels (>10  
12 ppm) is a major drawback since it poisons the electrodes in the fuel cell [21]. In the NO<sub>x</sub>  
13 reduction, however, the effect of CO is not necessarily negative. Furthermore, production of  
14 hydrogen in a fuel reformer causes a fuel penalty, which, together with the need for a reducing  
15 agent in the LNR unit (*i.e.* fuel), should be minimized in order to maintain high fuel economy.  
16 Many studies in the literature reports on the effect of hydrogen on the NO<sub>x</sub> reduction over the  
17 silver-alumina system, and often the hydrogen concentration is high (ranging between 1000 ppm  
18 and 1 vol%) [22]. One possible side effect of hydrogen addition to the silver-alumina catalyst is  
19 the formation of ammonia, which is mainly considered as negative, as ammonia is harmful for the  
20 environment. However, attempts have been made in order to use the formed ammonia in a NH<sub>3</sub>-  
21 SCR catalyst after the HC-SCR catalyst. The concept has been shown by DiMaggio et al. [23],  
22 where remaining NO<sub>x</sub> species are reduced by the ammonia formed over the HC-SCR catalyst.  
23

1 The aim of the present study is to investigate how various parameters, such as hydrogen and  
2 carbon monoxide concentration, affects the NO<sub>x</sub> reduction over the silver-alumina system. This  
3 work takes a system approach where parameters as temperature and fuel penalty are considered.  
4 Furthermore, realistic gas mixtures from exhaust and reformer are used in the experiments and  
5 the catalysts are coated on monolith samples to mimic a real system.

6

## 7 **2. Experimental**

### 8 2.1 ATR catalyst preparation

9 Table 1 shows the washcoat properties of the support and the RhPt-based catalyst used for the  
10 ATR experiments. The metal precursors used for the catalyst preparation were Rh nitrate  
11 (Rh(NO<sub>3</sub>)<sub>3</sub>, Rh 8-10 % w/w, Sigma Aldrich), Pt nitrate ((NH<sub>3</sub>)<sub>4</sub>Pt(NO<sub>3</sub>)<sub>2</sub>, Pt 3-4 % w/w, Alfa  
12 Aesar), Ce nitrate (Ce(NO<sub>3</sub>)<sub>3</sub>·6H<sub>2</sub>O, 99.99 %, Alfa Aesar) and La nitrate (La(NO<sub>3</sub>)<sub>3</sub>·6H<sub>2</sub>O, 99.9  
13 %, Alfa Aesar) solutions. The catalyst was supported on δ-alumina. The δ-alumina was made by  
14 calcining γ-alumina (PURALOX HP-14/150, Sasol Germany GmbH) at 1000 °C for 1 h with  
15 little loss of surface area. The alumina powder was impregnated with the metals by the incipient  
16 wetness (IW) technique in accordance to the nominal weight loading presented in Table 1. The  
17 resulting powders were calcined at 800 °C for 3 h and deposited via ethanol-slurry dip-coating  
18 procedure onto 400 cpsi cordierite monoliths, with dimensions OD=17.8 mm, l=30.5 mm  
19 (Corning).

20

### 21 2.2 ATR catalyst characterization

22 Fresh powder samples of Rh<sub>1.0</sub>Pt<sub>1.0</sub>Ce<sub>10</sub>La<sub>5.0</sub>/δ-Al<sub>2</sub>O<sub>3</sub>, taken from the catalyst preparation prior to  
23 the deposition on the monoliths, were characterized by using the following instruments: Surface  
24 area and pore size distribution were measured by nitrogen sorption at 77K using a Micromeritics

1 ASAP 2010 instrument. Approximately 0.4 g powder was used and degassed at 250°C for 3 h  
2 prior to analysis.

3  
4 The crystal phases were determined by X-ray diffraction (XRD), using a Siemens Diffraktometer  
5 D5000 scanning  $2\theta$  from 10°-90° in the scan mode (0.02°, 1s), using Ni filtered Cu-K $\alpha$  radiation.

6 Temperature programme reduction (TPR) was performed at 30-1000°C, 10°C/min, with  
7 hydrogen as adsorbate using a Micromeritics Autochem 2910 equipped with a TCD.

8 Approximately 0.1 g powder was used for the analysis.

9  
10 The surface composition and chemical state of the deposited additives and loaded active metals  
11 were determined using X-ray photoelectron spectroscopy (XPS). The XPS studies were  
12 performed in a Phi Quantum 2000 system.

13

#### 14 2.3 ATR experiments

15 The diesel reforming experiments were carried out at reactor inlet temperature of 650 °C and  
16 atmospheric pressure. A standard diesel fuel (~C/H=6.43 (weight ratio), ~6 ppm S,) whose  
17 physical and chemical properties are in close correlation to Swedish Environmental Class 1 diesel  
18 (MK 1) [24], was used as feedstock. The following operating parameters were employed:

19  $H_2O/C=3.0$ ,  $O_2=0.49$  ( $\lambda=0.33$ ), GHSV~17700 h<sup>-1</sup> and time on stream (TOS) ~3h. The

20 experiments were carried out in a vertically mounted stainless steel tubular reactor with ID=23.7

21 mm equipped with three thermocouples. The product gases were analyzed using a Gaset Cr-200

22 Fourier Transform Infrared Spectroscopy (FTIR) and a Maihak modular system S710 equipped

23 with non-dispersive infrared sensor (NDIR) and thermal conductivity detector (TCD).

24

## 1 2.4 LNR sample preparation

2 The LNR catalyst samples were prepared via wet impregnation and two single step sol-gel  
3 methods, as described previously [25]. The wet impregnation was performed by adding an  
4 Ag/EDTA-complex solution to a water based  $\gamma$ -Al<sub>2</sub>O<sub>3</sub> slurry (SBa200, Sasol), which was kept  
5 under stirring for 2 hours (AgNO<sub>3</sub> ( $\geq$ 99%, Sigma-Aldrich) as precursor) while the pH was kept at  
6 6.3 by nitric acid (10 %, Fluka) addition. The slurry was subsequently freeze-dried and calcined  
7 at 600°C. In the sol-gel methods, aluminum isopropoxide (AIP; 98+%, Aldrich) and silver nitrate  
8 were used as precursors. The formed gel was subsequently dried (thermally at 100 °C or by  
9 freeze-drying) followed by calcination at 600°C, and was then crushed to a fine powder. All  
10 samples were washcoated onto monoliths (400 cpsi, length 20 mm, 21 mm OD), using 20 wt%  
11 boehmite as binder. Further details about the preparation methods and the washcoating have been  
12 presented previously [25].

13  
14 To activate the hydrocarbon for NO<sub>x</sub> reduction in the SCR reaction, it is necessary to partially  
15 oxidize the hydrocarbon [12]. Platinum is a known oxidation catalyst, and can thus act as  
16 oxidation sites on the catalyst. However, the oxidation must be mild enough not to combust the  
17 reductant, but high enough to partially oxidize the hydrocarbon, preferably at low temperatures  
18 (below 300 °C). To achieve these properties of the catalyst, a minute amount of Pt (100 ppm by  
19 weight) was added to a catalyst containing 2 wt% Ag (nominal) prepared by sol-gel with freeze-  
20 drying. The platinum was added as a diluted (1000 ppm Pt by weight) platinum nitrate solution to  
21 the sol, one hour before gelling. Sol-gel with subsequent freeze-drying has been shown to highly  
22 distribute the metal throughout the alumina matrix [25], which is believed to promote the desired  
23 properties of the catalyst.

24



1 The specific surface areas of the samples were measured by nitrogen sorption at 77 K, using a  
2 Micromeritics Tristar instrument. The results are summarized in Table 2, together with the  
3 nominal metal content. The samples were denominated according to Table 2.

4  
5 A thorough characterization of the different LNR catalyst samples was performed in ref. [25].  
6 The amount of Pt in the Pt containing sample (2% AgPt100) was too low to be detected by the  
7 techniques applied in ref. [25]. Nevertheless, this sample showed similar characteristics as the  
8 corresponding silver-alumina sample without Pt addition.

#### 9 10 2.5 LNR performance

11 Two similar flow reactor systems were used for evaluation of the catalytic performance of the  
12 samples. The reactors consisted of a horizontal quartz tube heated by a heating coil, where the  
13 temperature was measured by two thermocouples (type K), 15 mm before the sample and inside  
14 the monolith sample (just before the rear end), respectively. Two uncoated 400 CPSI cordierite  
15 monoliths were placed before and after the sample monolith, respectively, to screen the  
16 thermocouples from radiation from the heating coil (first monolith) and to prevent heat losses via  
17 radiation from the back of the sample monolith (second monolith). The inlet gas composition was  
18 controlled by mass flow controllers from Bronkhorst High-Tech. Both reactors outlet gas  
19 composition was analyzed by an MKS 2000 FTIR instrument. *n*-octane and water were  
20 introduced separately to the reactors via controlled evaporator mixer (CEM) systems from  
21 Bronkhorst High-Tech. Overall, the differences between the reactor systems were negligible.

22  
23 The samples were pre-oxidized in 10% O<sub>2</sub> (Ar bal.) at 550°C for 20 minutes prior to the  
24 measurements. The measurements were carried out at steady state conditions at 200 °C, 250 °C

1 and 300 °C with a space velocity (GHSV) corresponding to 33 300 h<sup>-1</sup>. The inlet gas composition  
2 was set to 200 ppm NO, 5% H<sub>2</sub>O, 6% CO<sub>2</sub> and 10% O<sub>2</sub> (Ar bal.). To monitor the influence of the  
3 addition of reformat gas to the feed, the CO and H<sub>2</sub> concentrations were varied. The H<sub>2</sub>  
4 concentration was varied between 0 and 1000 ppm, while the CO concentration was varied  
5 between 350 and 850 ppm. At 250 °C, additional H<sub>2</sub> and CO concentrations of 3000 ppm and  
6 1850 ppm, respectively, were also introduced. This was to simulate different reformat gas feeds  
7 and to investigate the need for an on-board CO clean-up equipment. *n*-octane was used as  
8 reducing agent and the C/N ratio was varied between 3 and 12. At 250 °C an additional C/N ratio  
9 of 8 was included in order to investigate the influence of the C/N ratio at low temperatures in  
10 more detail.

11  
12 For some runs, an error in the program controlling the MFCs caused a faulty argon balance,  
13 leading to a somewhat decreased concentration of the inlet gases. This error mainly affected the  
14 NO, CO and H<sub>2</sub> concentration and the overall space velocity, especially for the cases with 3000  
15 ppm H<sub>2</sub> in the feed. However, the molar flow of all gases (except argon) remained constant. The  
16 conversion of NO<sub>x</sub> was therefore calculated from the real inlet concentration for the affected  
17 cases. The increase in space velocity was always less than 7.5 % and thereby considered to have a  
18 minor effect on the NO<sub>x</sub> conversion. This increase in space velocity was therefore neglected in  
19 the calculations. Based on the calculated results it was concluded that the erroneous argon  
20 balance did not significantly affect the discussion and conclusions of this study.

21

## 22 **3. Results**

### 23 3.1 ATR catalyst characterization results

1 The surface area and porosity results from the N<sub>2</sub>-BET measurements of the Rh<sub>1.0</sub>Pt<sub>1.0</sub>Ce<sub>10</sub>La<sub>5.0</sub>/δ-  
2 Al<sub>2</sub>O<sub>3</sub> sample are presented in Table 1. As seen in Table 1, the addition of the active metal and  
3 promoters reduced the surface area, the pore volume and the pore diameter of the δ-alumina  
4 support. The surface area of the thermal treated δ-alumina was ~105 m<sup>2</sup>/g while for the  
5 impregnated RhPt-sample it was 88 m<sup>2</sup>/g.

6  
7 The XRD pattern of the catalyst showed that the δ-phase of alumina was present for the fresh  
8 powder sample. Furthermore, only diffraction peaks from ceria and the support material were  
9 observed. This indicates that the rhodium and platinum particles are small and well dispersed in  
10 the washcoat. Peaks ascribed to fluorite-structured CeO<sub>2</sub> [26] were found at 2θ= 28.5, 48.5 and  
11 56.5°. The average crystallite size of ceria was ~8.0 nm.

12  
13 The TPR profile of Rh<sub>1.0</sub>Pt<sub>1.0</sub>Ce<sub>10</sub>La<sub>5.0</sub>/δ-Al<sub>2</sub>O<sub>3</sub> revealed three positive peaks. One major peak  
14 located at 150 °C, while the other was smaller and found at 450 and 900 °C, respectively. The  
15 reduction peak present at 150 °C is ascribed to reduction of bulk rhodium oxides species Rh<sub>x</sub>O<sub>x</sub>  
16 [27], the peak at 450 °C is owing to hydrogen spillover effect in the alumina support [27], while  
17 the peak at 900 °C is attributed to cerium oxides [28]. Platinum and lanthanum oxides were not  
18 detected by TPR.

19  
20 XPS measurements provided valuable information of the surface composition and oxidation state  
21 of the fresh catalyst (Table 3). Rhodium was found to be present in its oxidized state with a  
22 binding energy of 308.8 eV [29]. For platinum, the Pt(4d) peaks occur at about 314.0 eV which is  
23 metallic [29]. For ceria, the binding energy of the Ce 3d<sub>5/2</sub> line is found at 881.8 eV, indicating

1 CeO<sub>2</sub> [29]. The XPS survey spectra shows that La(3d) peaks is found at ~834.2 eV with a La/Al  
2 ratio of 0.091 indicating that La is in the dispersed phase [30].

3

### 4 3.2 ATR catalyst performance.

5 The performance of the catalyst using standard diesel as feedstock at reaction conditions  
6 H<sub>2</sub>O/C~3.0 and O<sub>2</sub>/C~0.49 are presented in Table 4. The activity results show that the  
7 washcoated monolith with the composition Rh<sub>1.0</sub>Pt<sub>1.0</sub>Ce<sub>10</sub>La<sub>5.0</sub>/δ-Al<sub>2</sub>O<sub>3</sub> is capable of providing a  
8 high diesel conversion, ~99%. The CO<sub>2</sub> selectivity expressed as the ratio CO<sub>2</sub>/(CO<sub>2</sub>+CO) was  
9 also high, just above 50%. The hydrogen concentration was 36 %. The measured hydrocarbon  
10 concentrations in the reformat were low. The methane concentration was ~600 ppm, while the  
11 ethylene concentration was ~300 ppm. No ethane, propane nor higher hydrocarbons were  
12 detected in the product gas. Also, very low amounts (total <10 ppm) of benzene, toluene and  
13 sulfur dioxide were detected by the FTIR and NDIR measurements.

14

15 The activity results from the Rh<sub>1.0</sub>Pt<sub>1.0</sub>Ce<sub>10</sub>La<sub>5.0</sub>/δ-Al<sub>2</sub>O<sub>3</sub> were used as a basis for the deNO<sub>x</sub>  
16 experiments, which are discussed in detail in the following sections.

17

### 18 3.3 LNR performance - Influence of feed composition

#### 19 *3.3.1 Influence of C/N ratio and CO feed concentrations*

20 The LNR performance for the catalyst samples, in the absence of hydrogen, was evaluated at 200,  
21 250 and 300 °C with the C/N ratios of 3 and 12, respectively, and different CO inlet  
22 concentrations (350 or 850 ppm). It is clear that without the addition of hydrogen no significant  
23 activity was observed below 300 °C, except for a slight NO<sub>x</sub> conversion (<5 %) for the high load  
24 (5%Ag and Mix) samples at 250 °C and C/N=12. At 300 °C however, most samples clearly show

1 the reduction of NO<sub>x</sub> (2%AgPt100 excepted). In general, the CO concentration did not show any  
2 promotional influence on the NO<sub>x</sub> conversion, regardless of temperature, in accordance to the  
3 results of e.g. Bogdanchikova et al. [31] and Breen et al. [32]. Overall, the results showed no  
4 significant effect of the CO concentration in the feed. Without the addition of hydrogen in the  
5 NO<sub>x</sub> conversion experiments, differences owing to the C/N ratio were hardly observable at  
6 temperatures below 300 °C and then only for the high load samples. Nevertheless, at 300 °C the  
7 increase in NO<sub>x</sub> conversion for these samples were considerable, from 13 % to ca 46 % (5%Ag)  
8 and from ca 15 % to ca 55 % (Mix), at C/N=3 and 12, respectively. The low loaded samples  
9 (2%Ag and 2%AgPt100) did not show any significant increase in NO<sub>x</sub> conversion due to changes  
10 in the C/N ratio at 300 °C: The 2%Ag sample showed a NO<sub>x</sub> conversion of about 16 %, while the  
11 2%AgPt100 sample always showed less than 10 % NO<sub>x</sub> conversion at these conditions.

12

### 13 3.3.2 Addition of hydrogen

14 The addition of 1000 ppm of hydrogen to the feed (Figure 1) results in an instant increase in NO<sub>x</sub>  
15 conversion, as frequently reported in the literature since the work of Satokawa [17]. The effect of  
16 the added hydrogen is clearly dependent on the temperature, as the difference in NO<sub>x</sub> conversions  
17 with and without hydrogen added is generally larger at higher temperatures. However, evaluating  
18 the individual results for the samples, there are exceptions: For C/N=3 and 250 °C, the high load  
19 samples show a slightly lower NO<sub>x</sub> conversion with H<sub>2</sub> in the feed than at 200 °C. Nevertheless,  
20 the differences are small and fall within experimental errors. For C/N=3, the largest difference in  
21 NO<sub>x</sub> conversion owing to H<sub>2</sub> addition is shown by the 2%Ag sample at 300 °C, increasing from  
22 around 17 % to 61 %. For C/N=12 however, the largest differences are shown for the Mix sample  
23 at 250 °C, increasing from ca 8 % to 74 %, but also (and more notably) for the 2%AgPt100  
24 sample at 300 °C, increasing from around 7 % to almost 88 %, a more than 12-fold increase in

1 NO<sub>x</sub> conversion. At 300 °C, it is observed that the 2%Ag sample does not seem to be affected by  
2 the change in C/N ratio, while on the other hand it has a considerable impact on the 2%AgPt100  
3 sample.

4

### 5 *3.3.3 Influence of hydrogen feed concentration*

6 According to the results in Figure 1, the lowest temperature showing any significant NO<sub>x</sub>  
7 conversion is 250 °C, with C/N=12. To increase the NO<sub>x</sub> conversion at this temperature within  
8 the limits of the reformer, 3000 ppm of hydrogen was added to the feed. Also, an additional  
9 intermediate C/N ratio of 8 was added to investigate the possibility of somewhat lowering the  
10 fuel penalty while maintaining a high NO<sub>x</sub> conversion. The CO feed was accordingly varied  
11 between 350 ppm and 1850 ppm, simulating a reforming system with and without CO clean-up.  
12 The results are shown in Figure 2.

13 At C/N=3 with 350 ppm CO and 3000 ppm H<sub>2</sub>, the high load samples show a slight increase in  
14 NO<sub>x</sub> conversion, from about 18 % to ca 24 % for both samples, compared to 1000 ppm H<sub>2</sub> and  
15 350 ppm CO in the feed (Table 6). The 2%Ag and 2%AgPt100 samples show a somewhat larger  
16 increase in NO<sub>x</sub> conversion from 18 % or 21 % with 1000 ppm H<sub>2</sub>, to 32 % and 38 %,   
17 respectively, with 3000 ppm H<sub>2</sub> in the feed. It is observed that the low load samples both show  
18 higher NO<sub>x</sub> conversion than the high load samples at these conditions. The increase of the CO  
19 feed concentration from 350 ppm to 1850 ppm (Figure 2) seems to have a slightly positive effect  
20 on the overall NO<sub>x</sub> conversion at these conditions, showing an increase with approximately 3-6  
21 percentage units for all samples.

22

23 For C/N=12 at 250 °C, the increase in hydrogen concentration results in a significant increase in  
24 NO<sub>x</sub> conversion for all samples, comparable with the results at 300 °C with 1000 ppm H<sub>2</sub> in the

1 feed (Figure 1, top right). In contrast to C/N=3, the CO feed concentration does not affect the  
2 NO<sub>x</sub> conversion at C/N=12 in any other significant way but slightly negative (Figure 2).  
3 Comparing C/N=12 and C/N=8 (Figure 2) with 350 ppm CO, the NO<sub>x</sub> conversion drops from 82  
4 % to 61 % for the 5%Ag sample and from 91 % to 67 % for the Mix sample. However, for the  
5 2%Ag sample the drop in NO<sub>x</sub> conversion is smaller, from 64 % to 57 %, and for the 2%AgPt100  
6 the drop is merely five percentage units, from 80 % to 75 %. Increasing the CO feed  
7 concentration at C/N=8 have no significant effect on the 2%Ag and 2%AgPt100 samples,  
8 however, a slight promotion of the NO<sub>x</sub> conversion over the 5%Ag (61 % vs. 66 %) and Mix (67  
9 % vs. 71 %) samples is observed.

10

### 11 3.4 NH<sub>3</sub> formation

12 The formation of nitrogen containing species, such as isocyanate, isocyanide and ammonia,  
13 during the HC-SCR reaction is well known and has been extensively reported [23, 33-38] and  
14 hydrogen has been shown to promote the formation of such species [23, 33, 34, 36, 38]. In this  
15 study, we observe the formation of ammonia (Table 5), especially with the addition of hydrogen  
16 to the feed (Figure 3), in accordance with the literature.

17

18 The ammonia is formed during the HC-SCR reaction under certain conditions. According to the  
19 results presented in Table 5, where no hydrogen is added to the feed, the only significant  
20 formation of ammonia is observed for the high load samples at 300 °C and a C/N ratio of 12.  
21 Notably, the amount of ammonia formed corresponds to about 20-25 % of the converted NO<sub>x</sub> at  
22 these conditions. A small amount of formed ammonia is also observed at 200 °C for these  
23 samples. However, considering the low NO<sub>x</sub> conversion at these conditions, these results should  
24 be regarded as possible artifacts, based on the fact that the formed ammonia would, in that case,

1 correspond to almost 100 % of the converted  $\text{NO}_x$ , which is highly unlikely. On the other hand,  
2 we were not able to directly measure the formation of  $\text{N}_2$  during the experiments, while it is not  
3 possible to entirely rule out this scenario. Figure 3 show the ammonia formation over the  
4 catalytic samples at different temperatures and C/N ratios when 1000 ppm hydrogen is added to  
5 the feed. At C/N=3 the formation of ammonia is very low, regardless of temperature, despite a  
6  $\text{NO}_x$  conversion between 30 % and 60 % for the different samples at 300 °C. At C/N=12  
7 however, a significant formation of ammonia can be observed over the high loaded samples at all  
8 temperatures, especially at 300 °C with over 50 ppm of formed ammonia over both samples.  
9 Most notable is the formation of ammonia over the high load samples at 200 °C, occurring at a  
10  $\text{NO}_x$  conversion of 21 % (5%Ag) and 26 % (Mix). The low loaded samples show a low ammonia  
11 formation overall, also for the high C/N ratio of 12. Only at 300 °C the 2%AgPt100 sample show  
12 any significant formation of ammonia (~14 ppm), while the ammonia formation over the 2%Ag  
13 sample never exceeds 10 ppm.

14  
15 Figure 4 shows the ammonia formation at 250 °C with 3000 ppm  $\text{H}_2$  added to the feed, also  
16 including the additional C/N ratio of 8. The low loaded samples still show a very low formation  
17 of ammonia at all conditions. The high loaded samples on the other hand, show an increase in  
18  $\text{NH}_3$  formation in comparison to 1000 ppm  $\text{H}_2$  in the feed and C/N=12 (Figure 3, middle right). A  
19 slight increase is also shown at C/N=3 for these samples. At C/N=8 and 3000 ppm  $\text{H}_2$ , the 5%Ag  
20 sample actually shows a slight increase in  $\text{NH}_3$  formation compared to C/N=12 with 1000 ppm  
21  $\text{H}_2$  in the feed, while the Mix samples show almost the same  $\text{NH}_3$  formation comparing the same  
22 conditions. From the results in Figure 3 and Figure 4 we cannot observe any impact owing to the  
23 CO concentration regarding the ammonia formation. Not even the considerable increase from 350



1 ppm to 1850 ppm CO when adding 3000 ppm H<sub>2</sub> to the feed shows any significant effect on the  
2 NH<sub>3</sub> formation.

3

#### 4 *3.4.1 Dual SCR system*

5 One possible way to make use of the formed ammonia is to add a NH<sub>3</sub>-SCR catalyst after the  
6 HC-SCR catalyst. The concept has been shown by DiMaggio et al. [23], where remaining NO<sub>x</sub>  
7 species are reduced by the ammonia formed over the HC-SCR catalyst. To investigate the impact  
8 of such a system, we calculated the total NO<sub>x</sub> reduction according to the following assumptions:

9

- 10 1. All NO in the gas feed that is converted over the HC-SCR catalyst forms either N<sub>2</sub> or  
11 NH<sub>3</sub>.
- 12 2. All ammonia that is formed over the HC-SCR catalyst is available as reducing agent for  
13 the NO reduction over the NH<sub>3</sub>-SCR catalyst, in the ratio 1:1.

14 The results are presented in Table 6.

15

## 16 **4. Discussion**

### 17 4.1 Fuel reforming

18 The activity results (Table 4) at ATR reaction conditions H<sub>2</sub>O/C ~ 3.0 and O<sub>2</sub>/C ~ 0.49 show that  
19 the Rh<sub>1.0</sub>Pt<sub>1.0</sub>Ce<sub>10</sub>La<sub>5.0</sub>/δ-Al<sub>2</sub>O<sub>3</sub> catalyst is highly active and capable of catalytically reforming the  
20 molecules in the diesel fuel to obtain close to complete fuel conversion. This feature is positive as  
21 a good fuel economy is crucial for diesel trucks, (see also section 4.4). Fuel slip from the  
22 reformer can deactivate the fuel cell e.g. in a polymer electrolyte fuel cell (PEFC) based APU  
23 system. The long hydrocarbon chains in diesel can easily get attached in the pores of the  
24 membranes, hindering the transport of the hydrogen ions from the anode to the cathode side [39].

1 Fuel slip does not have a negative effect on the LNR performance. The high hydrogen  
2 concentration, ~36 vol%, noted in Table 4, is more than sufficient to provide both the PEFC and  
3 LNR units with enough H<sub>2</sub> for power generation and NO<sub>x</sub> reduction. In Table 4, the high CO<sub>2</sub>  
4 selectivity, ~52%, is also positive as high CO concentrations are known to deactivate PEFCs due  
5 to CO adsorption on the typically Pt-coated anode electrodes [21]. However, for the LNR unit our  
6 results show that CO has no significant effect on the NO<sub>x</sub> reduction performance. The activity  
7 results in Table 4 show that low methane and ethylene concentrations, 600 and 300 ppm,  
8 respectively, were detected in the reformat by the FTIR and NDIR units. In reforming,  
9 generating low level of ethylene concentration in the reformat is considered crucial as ethylene  
10 is a known coke precursor. A high ethylene concentration is often an indication of severe carbon  
11 deposition taking place on the catalyst [40, 41]. This is detrimental as this often leads to  
12 significant reduction of the diesel reforming catalyst long term performance as the active surface  
13 sites of the catalyst are blocked by various types of carbon deposits. Further, these short  
14 hydrocarbons are generally not active over Ag/Al<sub>2</sub>O<sub>3</sub> at the current temperatures [15], while a  
15 clean-up catalyst after the LNR unit is required to prevent HC-slip.

16  
17 The characterization results from the N<sub>2</sub>-BET, XRD, H<sub>2</sub>-TPR and XPS analyses (Table 1 and 3)  
18 show the presence of finely dispersed bulk rhodium oxides, metallic platinum, ceria and  
19 lanthanum on the delta phase generated alumina support. These states of the active metals and  
20 promoters are believed to improve the catalyst reforming activity, stability and durability. The  
21 effects of the Rh-Pt metal loading and the addition of Ce-La additives on delta alumina were  
22 studied and reported in previous work [42, 43]. It was noted that the amount of accessible  
23 rhodium oxides and the introduction of ceria and lanthana on the alumina support were crucial as  
24 these features had a significant positive effect on the X<sub>diesel</sub>, S<sub>CO2</sub> and H<sub>2</sub> formation during ATR

1 of diesel at reaction conditions  $H_2O/C \sim 2.5$  and  $O_2/C \sim 0.49$  [42, 43]. Furthermore, it was found  
2 that ceria-rhodium and ceria-platinum interactions enhanced the development of bulk  $RhO_x$   
3 species which was believed to improve the catalyst activity, in particular the fuel conversion.  
4 Also, ceria was found to reduce the ethylene concentration in the reformat.

5

#### 6 4.2 $NO_x$ conversion

7 The results without the addition of hydrogen show that the high load (5% Ag and Mix) samples  
8 have a significantly higher  $NO_x$  conversion than the low load (2% Ag and 2% AgPt100) samples  
9 at 300 °C and  $C/N=12$ . This higher activity is visible also at 250 °C and  $C/N=12$  for the same  
10 samples, however to a lesser degree than at 300 °C. Most notable though is the 2% Ag sample that  
11 shows a higher  $NO_x$  conversion at 300 °C and  $C/N=3$  (16 %) than both high load samples (14 %),  
12 let be that the differences are small. The activity then slightly decreases when the  $C/N$  ratio is  
13 increased. This implies that the surface of the 2% Ag sample is at least partially covered by the *n*-  
14 octane, blocking the active sites. This has been shown by e.g. Shimizu et al. [15]. The higher  
15 activity shown by the high load samples is attributed to the higher amount of oxidation sites  
16 (metallic silver particles) in the samples, according to results from a previous study by Kannisto  
17 et al. [25]. The higher number of oxidation sites on the sample surface can readily oxidize and/or  
18 partially oxidize the high amount of octane at  $C/N=12$  and 300 °C, which is crucial for a high  
19  $NO_x$  conversion. At  $C/N=3$  and 300 °C, the high number of oxidation sites may lead to  
20 combustion of the octane, decreasing the  $NO_x$  conversion. In this case ( $C/N=3$ ), the lower amount  
21 of oxidation sites in the 2% Ag sample can partially oxidize a higher fraction of the hydrocarbon,  
22 avoiding combustion, than the high loaded samples, which is also showed in the higher  $NO_x$   
23 conversion.

24

1 Adding 1000 ppm hydrogen to the feed results in an overall increase in NO<sub>x</sub> conversion (Figure  
2 1), but more importantly the results confirm the previous conclusions. At C/N=3 the overall NO<sub>x</sub>  
3 conversion is low at temperatures below 300 °C. At 300 °C though, the NO<sub>x</sub> conversion is  
4 increased with the 2%Ag sample again showing the highest activity. At C/N=12 the activity  
5 increases already above 200 °C, with the high load samples showing the highest NO<sub>x</sub> conversion.  
6 However, the 2%AgPt100 sample now shows an increased NO<sub>x</sub> conversion, especially at 300 °C,  
7 where it is comparable with the conversion of the high load samples, around 90 %. These results  
8 imply that the platinum dopant acts as an oxidation site able to partially oxidize the  
9 hydrocarbons, as discussed above. The lack of activity without the addition of hydrogen may be  
10 due to that the platinum most likely is in an oxidized state during these experiments: The samples  
11 were calcined in air and also pre-treated in 10 % oxygen at 500 °C for 20 minutes prior to each  
12 activity test. It is possible that the hydrocarbon reductant is not capable of reducing any oxidized  
13 platinum in the catalyst, while the addition of hydrogen, being a more reductive element, results  
14 in the formation of metallic platinum particles acting as oxidation sites. The low activity at  
15 C/N=3, 300 °C should then be due to combustion of the reductant, however due to the amount of  
16 CO<sub>2</sub> in the feed we were unable to distinguish the amount of formed CO<sub>2</sub> from this combustion.  
17  
18 Increasing the hydrogen feed to 3000 ppm at 250 °C results in even higher overall NO<sub>x</sub>  
19 conversion. Also, the differences in activity between the samples are decreased. However, similar  
20 trends as previously are observed, with the low loaded samples showing slightly higher activity  
21 than the high loaded samples at C/N=3. However, at C/N=8 and 12, the 2%Ag sample is showing  
22 the lowest NO<sub>x</sub> conversion, while the 2%AgPt100 sample shows similar activity as the high  
23 loaded samples, especially at C/N=8. There is a possibility that some NO<sub>x</sub> conversion over the  
24 2%AgPt100 sample may be due to H<sub>2</sub>-SCR over the platinum sites [44]. However, since the NO<sub>x</sub>

1 conversion increases with the C/N ratio, we draw the conclusion that the HC-SCR reaction  
2 constitutes the dominating part of the NO<sub>x</sub> conversion for the 2%AgPt100 sample. Also, any  
3 significant effect from the H<sub>2</sub>-SCR would have shown at 200 °C, which is not the case.

4  
5 The most important conclusion from this discussion is that to achieve an efficient HC-SCR  
6 catalyst, oxidation sites that can partially oxidize the reductant is required, as previously shown in  
7 the literature for pure Ag/Al<sub>2</sub>O<sub>3</sub> catalysts [12]. The results in the present study strongly imply that  
8 this can be achieved with other oxidation sites than silver, such as well dispersed trace amounts  
9 of platinum. Too great a number of oxidation sites will nevertheless naturally lead to combustion  
10 of the hydrocarbon reducing agent.

11

#### 12 4.3 NH<sub>3</sub> formation

13 Regarding the formation of ammonia, several obvious conclusions can be drawn from the results  
14 presented in Table 5, Figure 3 and Figure 4. First, the silver loading is crucial for the formation of  
15 NH<sub>3</sub>, as the low loaded samples show very low formation of NH<sub>3</sub>, virtually regardless of  
16 conditions. Both samples show less than 10 ppm of ammonia at all times, except for the  
17 2%AgPt100 sample at C/N=12 and 300 °C, showing an ammonia formation of about 14 ppm.  
18 The high load samples on the other hand, show a more significant NH<sub>3</sub> formation at C/N=12 and  
19 with addition of 1000 ppm H<sub>2</sub> (Figure 3), but also without H<sub>2</sub> addition at 300 °C (Table 5).  
20 Further, at C/N=8 and 12 with 3000 ppm H<sub>2</sub> (Figure 4) a notable amount of NH<sub>3</sub> is formed.  
21 Based on these results it seems as larger silver particles, present in the high load samples  
22 according to ref. [25], promote the formation of ammonia during the HC-SCR reaction. Notably,  
23 the formation of ammonia is not necessarily coupled to the NO<sub>x</sub> conversion. As an example, the  
24 NO<sub>x</sub> conversion is high over the low loaded samples at C/N=8 and 12, adding 3000 ppm H<sub>2</sub> to

1 the feed (Figure 2). However, the corresponding  $\text{NH}_3$  formation is low (Figure 4), in comparison  
2 to the results of the high load samples. These results imply that the  $\text{NH}_3$  formation does not occur  
3 over the same sites as the  $\text{NO}_x$  reduction to  $\text{N}_2$ . Also, the results strongly imply that a surplus of  
4 hydrocarbons is needed to achieve ammonia formation during the HC-SCR reaction. This is  
5 clearly shown in Figure 3 and Figure 4, as the formation of  $\text{NH}_3$  at  $\text{C/N}=3$  is very low over all  
6 samples and at all conditions. Hydrogen addition and increased temperatures positively influence  
7 the  $\text{NH}_3$  formation, but the effect is only significant at high  $\text{C/N}$  ratios. This is consistent with the  
8 mechanisms for HC-SCR suggested in the literature. Eränen et al. [45] reported that ammonia is  
9 formed via isocyanate and isocyanide species. The formation of these species is promoted by the  
10 addition of hydrogen [36]. Conditions promoting a high formation of these isocyanate and  
11 isocyanide species, i.e. a high  $\text{C/N}$  ratio, addition of hydrogen and/or increased temperature,  
12 should be favourable for  $\text{NH}_3$  formation as shown by the results in the present study.

13

#### 14 *4.3.1 Dual SCR*

15 The  $\text{NH}_3$  formation results confirm the findings of DiMaggio et al. [23], that hydrogen plays a  
16 crucial role in the formation of ammonia, although the experiments in the present study was  
17 conducted at a lower temperature and hydrogen concentration than in ref. [23]. Further, the  
18 results calculated for our theoretical dual SCR system show that such a system could significantly  
19 increase the  $\text{NO}_x$  reduction efficiency compared to the HC-SCR system, showing a  $\text{NO}_x$   
20 reduction of ca 85 % for the Mix sample at 250 °C and  $\text{C/N}=12$ , provided that the assumptions  
21 stated for the calculation hold. Likely, all  $\text{NO}$  is not converted to  $\text{N}_2$  or  $\text{NH}_3$ , but also to other  
22 nitrogen-containing species such as  $\text{NO}_2$ , amines etc. In addition, for a commercial version of  
23 such a system, diesel would be used as reductant instead of *n*-octane, further reducing the

1 efficiency. However, the concept of a dual SCR is shown to be promising as a way of increasing  
2 the efficiency of the HC-SCR system.

3

#### 4 4.4 Fuel penalty

5 In order to maintain a good fuel economy for the diesel engine it is important to minimize the  
6 fuel penalty for the NO<sub>x</sub> abatement. The NO<sub>x</sub> conversion efficiency of a HC-SCR system depends  
7 on the amount of diesel that is needed to meet the conversion requirements. In general, a large  
8 HC/NO<sub>x</sub> ratio leads to a high NO<sub>x</sub> conversion efficiency. The results presented in this work, and  
9 in previous work (e.g. [23]), indicate that HC/NO<sub>x</sub> ratio between 6 and 8 is sufficient for a high  
10 NO<sub>x</sub> conversion. This will lead to a fuel penalty of about 1.8 gram of diesel for each gram of NO<sub>x</sub>  
11 removed from the exhausts. However, in order to reach high LNR efficiency at low temperatures  
12 hydrogen needs to be added. In the present study different hydrogen concentrations have been  
13 used and about 1000 ppm of H<sub>2</sub> is a reasonable number in this respect. In the literature there are  
14 examples of studies where hydrogen concentrations up to 1 vol% (10 000 ppm) have been used,  
15 which would lead to unacceptable fuel penalties if utilized in real systems. A H<sub>2</sub> addition of 1000  
16 ppm would correspond to approximately 2 grams of diesel fuel. The total fuel penalty is therefore  
17 3.8 grams of diesel for each gram of NO<sub>x</sub> removed from the system. If the fuel consumption and  
18 NO<sub>x</sub> exhaust levels are assumed to be 200 g/kWh and 1 g/kWh, respectively, this is equivalent to  
19 a fuel penalty of about 2%.

20

21 For comparison, to reduce 1 gram of NO<sub>x</sub> using urea-SCR, which is the presently most efficient  
22 way to remove NO<sub>x</sub> in lean exhausts, 2 grams of urea-solution is required. The cost of urea is  
23 approximately half of the diesel cost (in Europe), which means that 1 gram of NO<sub>x</sub> reduction is  
24 equivalent to 1 gram of diesel fuel, and a fuel penalty of approximately 0.5%. Nevertheless, as

1 shown earlier in this study, a dual-SCR approach may lower the fuel penalty. However, further  
2 studies to optimize such a system are needed.

3

#### 4 **5. Conclusions**

5 This paper reports on high activity for lean NO<sub>x</sub> reduction, already at low temperatures, using  
6 silver-alumina based catalysts and realistic exhaust-gas conditions and addition of hydrogen, as  
7 produced in a reformer system.

8

9 A high C/N ratio and addition of hydrogen has a positive influence on the NO<sub>x</sub> conversion.  
10 However, as was seen for the 2%Ag sample, provided 1000 ppm of hydrogen is added to the  
11 feed, a relatively high NO<sub>x</sub> conversion can be achieved at a low C/N ratio, albeit at high  
12 temperature (300 °C). Adding trace amounts of platinum (100 ppm by weight) to the 2%Ag  
13 catalyst significantly increases the NO<sub>x</sub> conversion at high C/N ratios. Further addition of  
14 hydrogen also enhances the activity over the Pt doped catalyst, compared to the 2%Ag sample,  
15 also at lower C/N ratios. The results for the samples with high silver loading show similar trends  
16 as for the Pt doped catalyst, with high NO<sub>x</sub> conversion at high C/N ratios. This implies that  
17 platinum may act as oxidation site, needed for the partial oxidation of the reducing agent.

18

19 NH<sub>3</sub> formation is promoted by a high C/N ratio and hydrogen feed, but is not necessarily coupled  
20 to a high NO<sub>x</sub> conversion. A high NH<sub>3</sub> formation is observed only over the high loaded samples,  
21 while the low loaded samples consistently show a low NH<sub>3</sub> formation, regardless of NO<sub>x</sub>  
22 conversion. Thus, it is concluded that the NH<sub>3</sub> formation is promoted by high silver loading. The  
23 formed ammonia may be used in a dual SCR system to increase the total NO<sub>x</sub> reduction and to  
24 reduce the fuel penalty.



1  
2 It is shown that the production of hydrogen corresponding to 1000 ppm hydrogen addition to the  
3 feed results in an unacceptable fuel penalty, compared to urea-SCR. It is concluded that the  
4 amount of hydrogen added to the LNR must be reduced in real applications.

## 6 **Acknowledgements**

7 This work has been performed as part of the MISTRA programme E4 (Energy Efficient  
8 Reduction of Exhaust Emissions from Vehicles), at the Competence Centre for Catalysis (KCK),  
9 Chalmers University of Technology and at KTH - Royal Institute of Technology. KCK is  
10 financially supported by Chalmers University of Technology, the Swedish Energy Agency and  
11 the member companies: AB Volvo, Volvo Car Corporation, Scania CV AB, Saab Automobile  
12 Powertrain AB, Haldor Topsøe A/S and ECAPS. Financial support from MISTRA (The  
13 Foundation for Strategic Environmental Research), the Swedish Road Administration, and from  
14 the Knut and Alice Wallenberg Foundation, Dnr KAW 2005.0055, is gratefully acknowledged.

## 15 **References**

- 16 [1] N. Aoyama, K. Yoshida, A. Abe, T. Miyadera, *Catal. Lett.* 43 (1997) 249.  
17 [2] K.A. Bethke, H.H. Kung, *J. Catal.* 172 (1997) 93.  
18 [3] T.E. Hoost, R.J. Kudla, K.M. Collins, M.S. Chattha, *Appl. Catal., B* 13 (1997) 59.  
19 [4] H.W. Jen, *Catal. Today*. 42 (1998) 37.  
20 [5] K. Masuda, K. Tsujimura, K. Shinoda, T. Kato, *Appl. Catal. B: Environ.* 8 (1996) 33.  
21 [6] T. Miyadera, *Appl. Catal. B: Environ.* 2 (1993) 199.  
22 [7] T. Miyadera, *Appl. Catal. B: Environ.* 13 (1997) 157.  
23 [8] T. Miyadera, *Appl. Catal. B: Environ.* 16 (1998) 155.  
24 [9] S. Kameoka, Y. Ukisu, T. Miyadera, *PCCP*. 2 (2000) 367.  
25 [10] A. Keshavaraja, X. She, M. Flytzani-Stephanopoulos, *Appl. Catal. B: Environ.* 27 (2000) L1.  
26 [11] K. Shimizu, J. Shibata, H. Yoshida, A. Satsuma, T. Hattori, *Appl. Catal. B: Environ.* 30 (2001)  
27 151.  
28 [12] K. Shimizu, M. Tsuzuki, K. Kato, S. Yokota, K. Okumura, A. Satsuma, *J. Phys. Chem. C*. 111  
29 (2007) 950.  
30 [13] Y.B. Yu, H. He, Q.C. Feng, *J. Phys. Chem. B*. 107 (2003) 13090.  
31 [14] L.E. Lindfors, K. Eränen, F. Klingstedt, D.Y. Murzin, *Top. Catal.* 28 (2004) 185.  
32 [15] K. Shimizu, A. Satsuma, T. Hattori, *Appl. Catal. B: Environ.* 25 (2000) 239.  
33 [16] G.K. Boreskov, *Catalysis*. 3 (1982) 39.

- 1 [17] S. Satokawa, Chem. Lett. 29 (2000) 294.  
2 [18] M. Nilsson, X. Karatzas, B. Lindstrom, L.J. Pettersson, Chem. Eng. J. 142 (2008) 309.  
3 [19] A. Abu-Jrai, A. Tsolakis, A. Megaritis, Int. J. Hydrogen Energy. 32 (2007) 3565.  
4 [20] S. Sitshebo, A. Tsolakis, K. Theinnoi, International Journal of Hydrogen Energy. 34 (2009) 7842.  
5 [21] X. Cheng, Z. Shi, N. Glass, L. Zhang, J.J. Zhang, D.T. Song, Z.S. Liu, H.J. Wang, J. Shen, J.  
6 Power Sources. 165 (2007) 739.  
7 [22] R. Burch, Catal. Rev. -Sci. Eng. 46 (2004) 271.  
8 [23] C.L. DiMaggio, G. B. Fisher, K. M. Rahmoeller, M. Sellnau, SAE Special publication. SP-2254  
9 (2009) 47.  
10 [24] T.S.P. Institute, SPI, [www.spi.se](http://www.spi.se), last visited 2010-09-19  
11 [25] H. Kannisto, H.H. Ingelsten, M. Skoglundh, J. Mol. Catal. A: Chem. 302 (2009) 86.  
12 [26] S. Damyanova, J.M.C. Bueno, Appl. Catal. A. 253 (2003) 135.  
13 [27] C.P. Hwang, C.T. Yeh, Q.M. Zhu, Catal. Today. 51 (1999) 93.  
14 [28] H.C. Yao, Y.F.Y. Yao, J. Catal. 86 (1984) 254.  
15 [29] R. Polvinen, M. Vippola, M. Valden, T. Lepisto, A. Suopanki, M. Harkonen, J. Catal. 226 (2004)  
16 372.  
17 [30] L.P. Haack, J.E. Devries, K. Otto, M.S. Chattha, Appl. Catal. A. 82 (1992) 199.  
18 [31] N. Bogdanchikova, F.C. Meunier, M. Avalos-Borja, J.P. Breen, A. Pestryakov, Appl. Catal. B:  
19 Environ. 36 (2002) 287.  
20 [32] J.P. Breen, R. Burch, C. Hardacre, C.J. Hill, J. Phys. Chem. B. 109 (2005) 4805.  
21 [33] B. Wichterlova, P. Sazama, J.P. Breen, R. Burch, C.J. Hill, L. Capek, Z. Sobalik, J. Catal. 235  
22 (2005) 195.  
23 [34] J.P. Breen, R. Burch, C. Hardacre, C.J. Hill, C. Rioche, J. Catal. 246 (2007) 1.  
24 [35] N. Bion, J. Saussey, C. Hedouin, T. Seguelong, M. Daturi, PCCP. 3 (2001) 4811.  
25 [36] R. Burch, J.P. Breen, C.J. Hill, B. Krutzsch, B. Konrad, E. Jobson, L. Cider, K. Eränen, F.  
26 Klingstedt, L.E. Lindfors, Top. Catal. 30-31 (2004) 19.  
27 [37] F.C. Meunier, J.P. Breen, V. Zuzaniuk, M. Olsson, J.R.H. Ross, J. Catal. 187 (1999) 493.  
28 [38] P. Sazama, L. Capek, H. Drobna, Z. Sobalik, J. Dedecek, K. Arve, B. Wichterlova, J. Catal. 232  
29 (2005) 302.  
30 [39] G. Kolb, *Fuel Processing*, WILEY-VCH Verlag GmbH & Co. KGaA: Weinheim, 2008.  
31 [40] S. Yoon, I. Kang, J. Bae, Int. J. Hydrogen Energy. 33 (2008) 4780.  
32 [41] J.R. Rostrup-Nielsen, T.S. Christensen, I. Dybkjaer, Stud. Surf. Sci. Catal. 113 (1998) 81.  
33 [42] X. Karatzas, D. Creaser, A. Grant, J. Dawody, L.J. Pettersson, Catal. Today (2010) doi:  
34 10.1016/j.cattod.2010.10.019.  
35 [43] X. Karatzas, J. Dawody, A. Grant, E. Elm Svensson, L.J. Pettersson, Appl. Catal. B (2010) doi:  
36 10.1016/j.apcatb.2010.09.027.  
37 [44] R. Burch, M.D. Coleman, J. Catal. 208 (2002) 435.  
38 [45] K. Eränen, F. Klingstedt, K. Arve, L.E. Lindfors, D.Y. Murzin, J. Catal. 227 (2004) 328.  
39  
40

41

## 1 **Table captions**

2 **Table 1:** Washcoat properties for the powder support and catalyst (ATR) used in this study. For the  
3 powder catalyst, the subscripts in the molecular formula reveal the nominal weight loading of the active  
4 metals and promoters on the alumina support. The surface area and porosity were measured by N<sub>2</sub>-BET  
5 while the crystallite size of ceria was measured by XRD using the Scherrer equation at Bragg angle  
6  $2\theta=28.5^\circ$ .

7  
8 **Table 2:** Sample preparation methods, nominal silver loading and specific surface area for LNR catalyst  
9 samples.

10  
11 **Table 3:** Binding energies and surface atomic ratios for the fresh powder sample Rh<sub>1.0</sub>Pt<sub>1.0</sub>Ce<sub>10</sub>La<sub>5.0</sub>/ $\delta$ -  
12 Al<sub>2</sub>O<sub>3</sub>

13  
14 **Table 4:** Results for ATR of standard diesel fuel over catalyst Rh<sub>1.0</sub>Pt<sub>1.0</sub>Ce<sub>10</sub>La<sub>5.0</sub>/ $\delta$ -Al<sub>2</sub>O<sub>3</sub> at H<sub>2</sub>O/C=3.0,  
15 O<sub>2</sub>=0.49 ( $\lambda=0.33$ ), GHSV~17700 h<sup>-1</sup>.

16  
17 **Table 5:** NH<sub>3</sub> formation without hydrogen addition, for C/N=3 and C/N=12 with *n*-octane as reductant at  
18 200, 250 and 300 °C for 2%Ag, 2%AgPt100, 5%Ag and Mix samples. Inlet conditions: 200 ppm NO, 5%  
19 H<sub>2</sub>O, 6% CO<sub>2</sub> and 10% O<sub>2</sub> (Ar bal.). CO concentrations are stated in the table. GHSV=33, 300 h<sup>-1</sup>.

20  
21 **Table 6:** Calculated total NO<sub>x</sub> reduction for a theoretical dual SCR system. Gas feed over the HC-SCR  
22 catalyst: 200 ppm NO, 5% H<sub>2</sub>O, 6% CO<sub>2</sub> and 10% O<sub>2</sub> (Ar bal.), with A: 350 ppm CO or B: 850 ppm CO  
23 or C: 350 ppm CO, 1000 ppm H<sub>2</sub> or D: 850 ppm CO, 1000 ppm H<sub>2</sub>. C/N=12, with *n*-octane as reductant.  
24 GHSV=33, 300 h<sup>-1</sup>.

25

1 **Figure captions**

2

3 **Figure 1:** NO<sub>x</sub> conversion for C/N=3 (left) and C/N=12 (right) at 200, 250 and 300 °C with *n*-  
4 octane as reductant and 1000 ppm H<sub>2</sub> in the feed for 2% Ag (○), 2% AgPt100 (□), 5% Ag (+) and  
5 Mix (×) samples. Inlet conditions: 200 ppm NO, 1000 ppm H<sub>2</sub>, 5% H<sub>2</sub>O, 6% CO<sub>2</sub> and 10% O<sub>2</sub>  
6 (Ar bal.). CO concentrations are stated in the figure. GHSV=33, 300 h<sup>-1</sup>.

7

8 **Figure 2:** NO<sub>x</sub> conversion at 250 °C with *n*-octane as reductant and 3000 ppm H<sub>2</sub> in the feed for  
9 2% Ag (○), 2% AgPt100 (□), 5% Ag (+) and Mix (×) samples. Inlet conditions: 200 ppm NO, 3000  
10 ppm H<sub>2</sub>, 5% H<sub>2</sub>O, 6% CO<sub>2</sub> and 10% O<sub>2</sub> (Ar bal.). CO concentrations are stated in the figure.  
11 GHSV=33, 300 h<sup>-1</sup>.

12

13 **Figure 3:** NH<sub>3</sub> formation for C/N=3 (left) and C/N=12 (right) at 200, 250 and 300 °C with *n*-  
14 octane as reductant and 1000 ppm H<sub>2</sub> in the feed for 2% Ag (○), 2% AgPt100 (□), 5% Ag (+) and  
15 Mix (×) samples. Inlet conditions: 200 ppm NO, 1000 ppm H<sub>2</sub>, 5% H<sub>2</sub>O, 6% CO<sub>2</sub> and 10% O<sub>2</sub>  
16 (Ar bal.). CO and H<sub>2</sub> concentrations are stated in the figure. GHSV=33, 300 h<sup>-1</sup>.

17

18 **Figure 4:** NH<sub>3</sub> formation at 250 °C with *n*-octane as reductant and 3000 ppm H<sub>2</sub> in the feed for  
19 2% Ag (○), 2% AgPt100 (□), 5% Ag (+) and Mix (×) samples. Inlet conditions: 200 ppm NO, 3000  
20 ppm H<sub>2</sub>, 5% H<sub>2</sub>O, 6% CO<sub>2</sub> and 10% O<sub>2</sub> (Ar bal.). CO concentrations are stated in the figure.  
21 GHSV=33, 300 h<sup>-1</sup>.

**Figures**

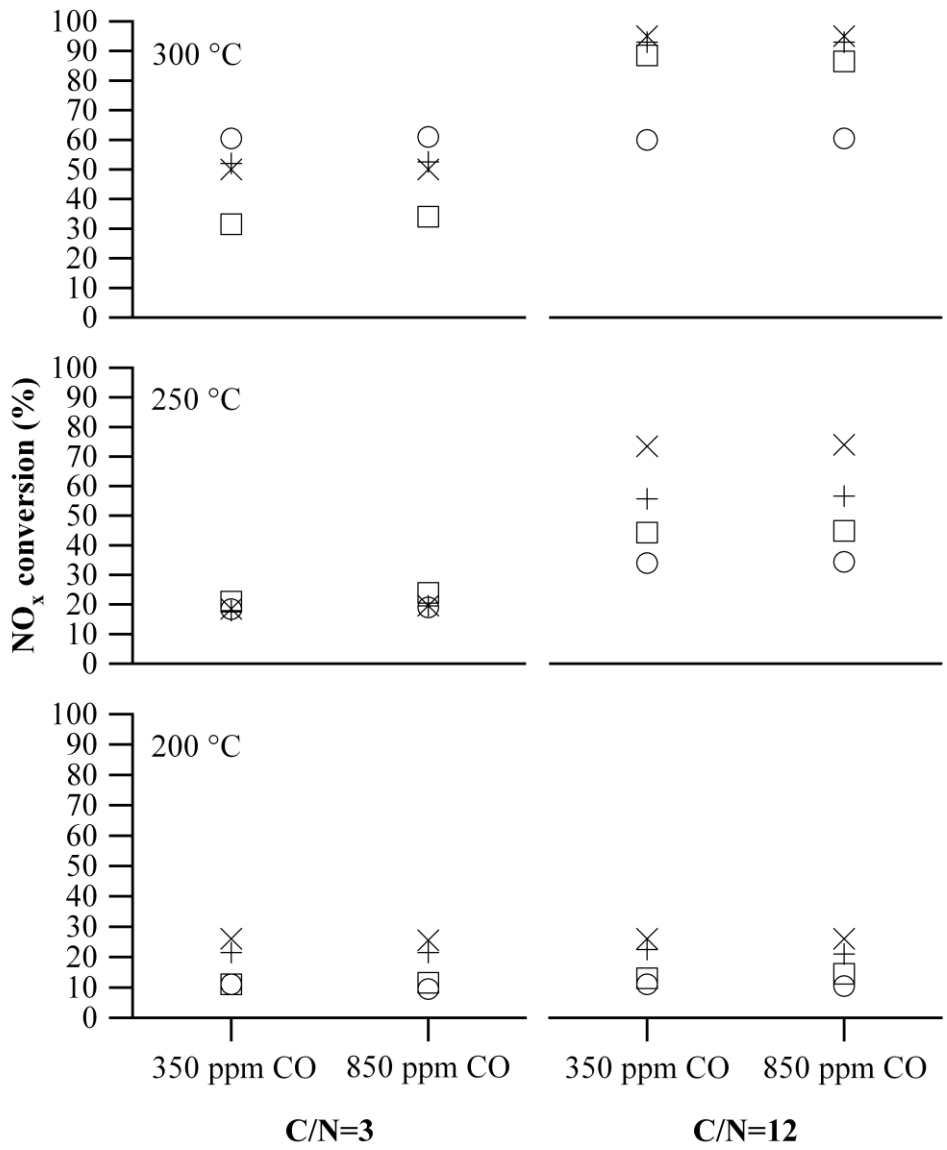


**Figure 1**

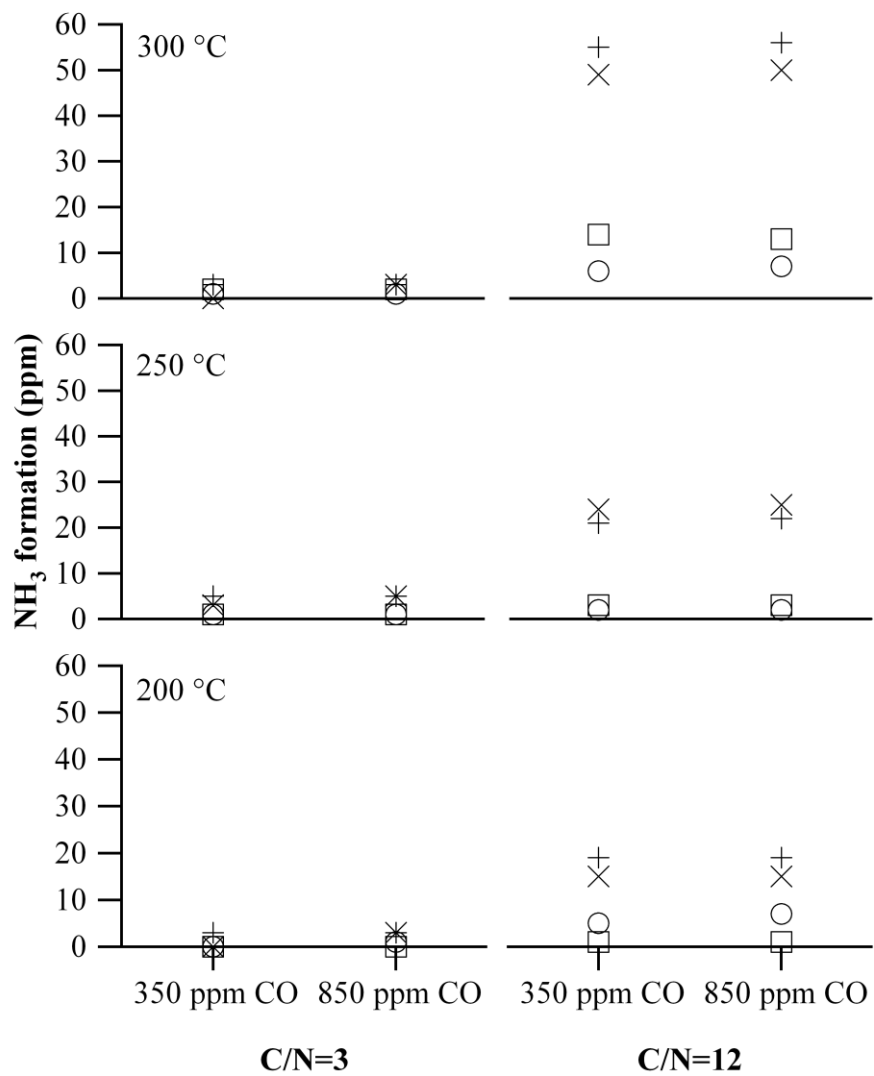
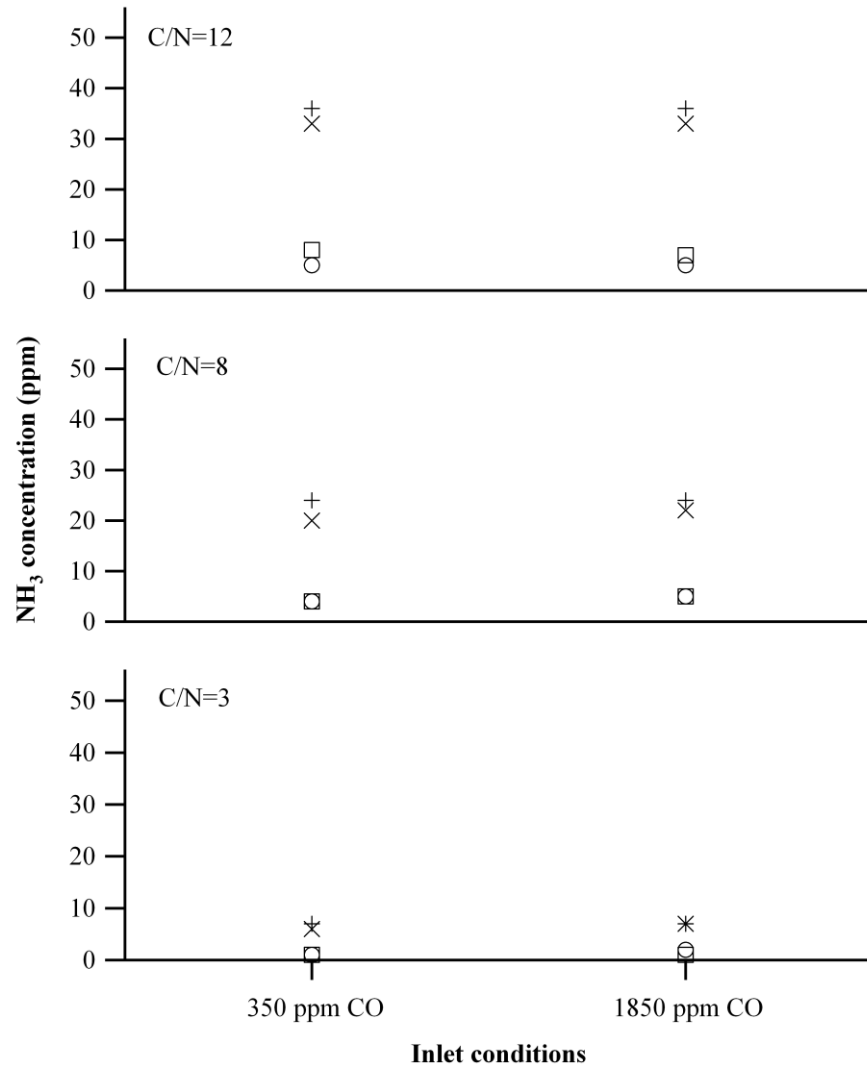
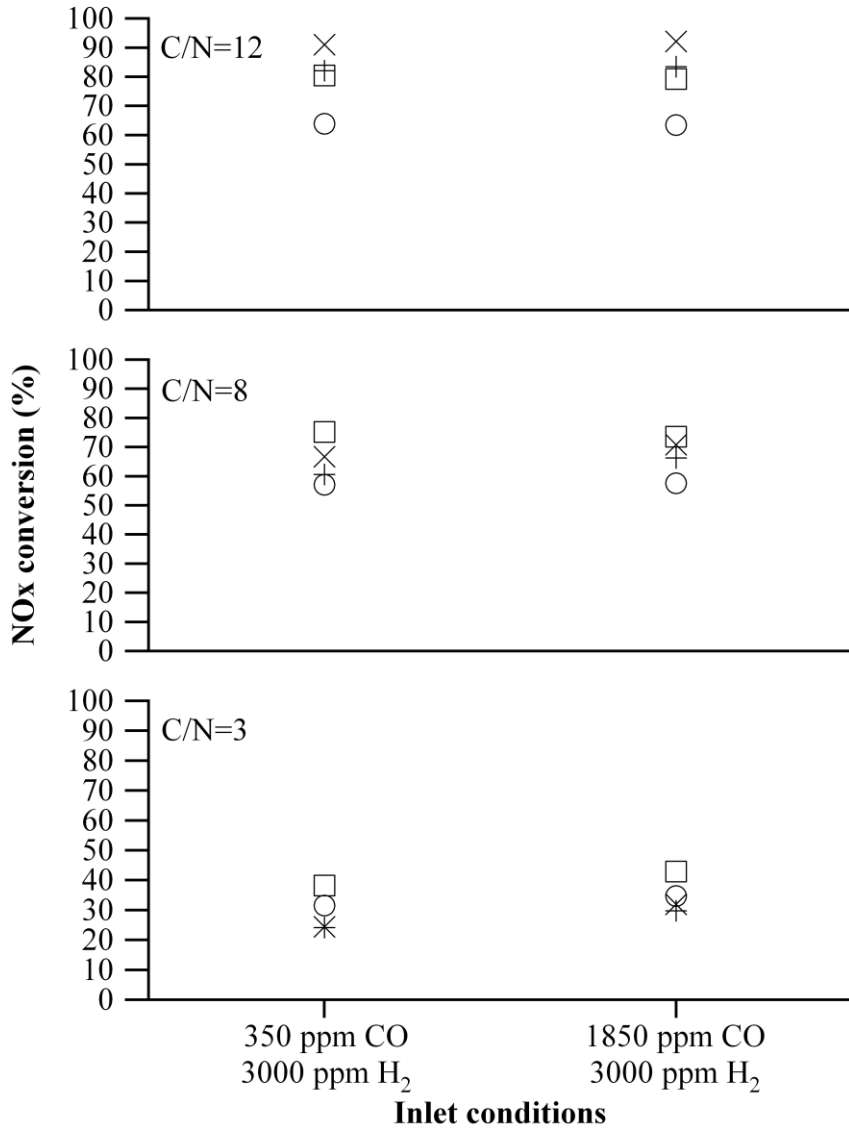


Figure 2



**Figure 3**



**Figure 4**